We are IntechOpen,
the world's leading publisher of
Open Access books
Built by scientists, for scientists

5,400
Open access books available

133,000
International authors and editors

165M
Downloads

154
Countries delivered to

Our authors are among the

TOP 1%
most cited scientists

12.2%
Contributors from top 500 universities

BOOK CITATION INDEX
CLARIVATE ANALYTICS
INDEXED

WEB OF SCIENCE™

Selection of our books indexed in the Book Citation Index
in Web of Science™ Core Collection (BKCI)

Interested in publishing with us?
Contact book.department@intechopen.com

Numbers displayed above are based on latest data collected.
For more information visit www.intechopen.com

Evaluation of Local Effects of Transitional Knudsen Number on Shock Wave Boundary Layer Interactions

R. Votta, G. Ranuzzi, M. Di Clemente, A. Schettino and M. Marini
CIRA Italian Aerospace Research Centre
Capua (CE),
Italy

1. Introduction

In the frame of the Italian aerospace research programme PRORA, two research activities are being performed in parallel, that are considered critical in the design of a re-entry vehicle: the evaluation of the Shock Wave - Boundary Layer Interaction (SWBLI) over a control surface and the analysis of rarefaction effects at high altitude. It is well known that on one side the SWBLI phenomenon strongly affects the efficiency of control surfaces during the re-entry, and on the other side the behavior of a hypersonic vehicle at high altitude is very different with respect to what happens in continuum regime, in particular for what concerns both the aerodynamic coefficients and the heat loads. Therefore, the correct evaluation of both phenomena is crucial in the design phase. The SWBLI phenomenon can be simulated in flight by means of advanced numerical codes, provided that a good accuracy of both the numerical scheme and the grid is attained; due to the high energy that typically characterizes the upper part of a re-entry path, the CFD code must be also capable to solve the Navier-Stokes equations taking into account chemical and vibrational non-equilibrium. Since a few experimental data are available for dissociated flows, in the frame of PRORA program some specific tests have been designed to validate the CIRA code H3NS; moreover, the goal of such experiments is to improve the understanding of the phenomenon, in order to be able to correlate flight and wind tunnel conditions and to extrapolate from flight and to flight the experimental data (Di Clemente et al., 2005).

However, since the stagnation pressure of a facility like the CIRA Plasma Wind Tunnel (PWT) Scirocco is very low with respect to a classic aerodynamic wind tunnel, a question arises about the possible rarefaction effects that can occur and that can influence the results of the tests; indeed the unit free-stream Knudsen number in Scirocco ranges from a value of $5.375*10^{-5}$ for the higher pressures, to a maximum of $1.467*10^{-3}$ in the lower pressure conditions (P0=1 bar); in **Fig. 1** the variation of Kn is reported as function of the reservoir pressure and enthalpy for both the nozzles D and F; these values could justify local rarefaction effects, for example over the nose, even though much of the flow domain is in continuum regime (Markelov et al., 2000).
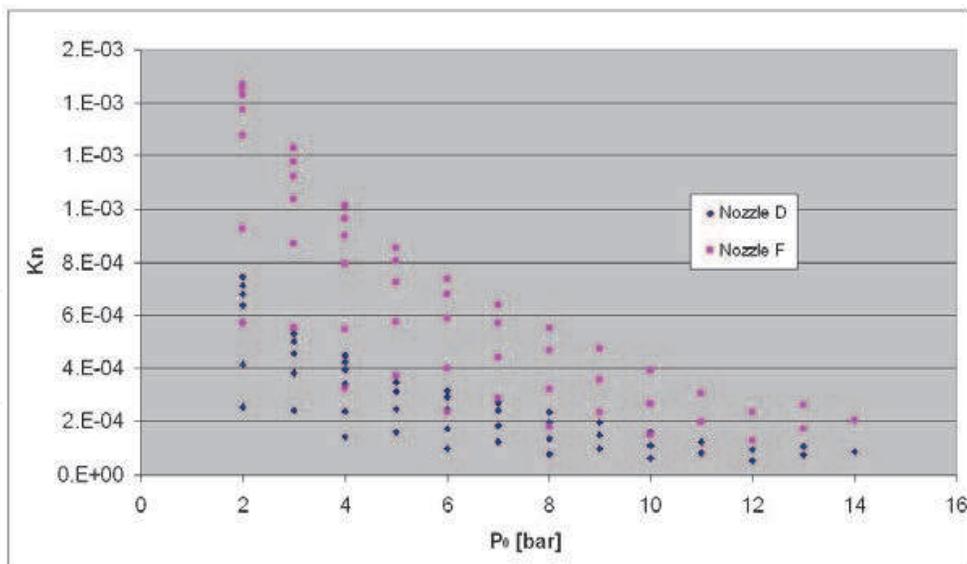
Fig. 1. Kn vs Reservoir pressure in Scirocco PWT.

Moreover, the SWBLI phenomenon itself can be affected by rarefaction effects (Markelov et al., 2000). Therefore, the same numerical tools that are typically used in flight to assess the rarefaction effects on the aerodynamic coefficients of a full vehicle have been used in wind tunnel conditions in order to verify if they occur in the experimental test. Two different tools are available at CIRA for this purpose: on one side, a DSMC code developed (Bird, 1995) for rarefied flows; on the other side, suitable slip flow conditions have been implemented in the H3NS CIRA code in order to allow the Navier-Stokes solver to deal with rarefied flows. Some details about both codes are given in the following section. In order to validate the code with the slip conditions, a classic numerical test case has been used, and the H3NS results have been compared with both numerical and experimental results (Markelov et al., 2000 and Marini, 2002). The comparisons were very satisfactory and are summarized in section 3.

Then, the same tools have been applied to rebuild the Scirocco tests, in order to check if rarefaction effects locally occur. The results are presented in section 3.

2. Numerical approaches

2.1 Navier-Stokes method

The continuum regime results have been obtained by using the CIRA Computational Fluid Dynamics (CFD) code H3NS developed at the Aerothermodynamics and Space Propulsion Laboratory by Ranuzzi et al. (2006). The code solves the full Reynolds Averaged Navier-Stokes (RANS) equations and considers the air flow in thermo-chemical non-equilibrium. Park model (1989) with five species (O, N, NO, O_2, N_2) and 17 chemical reactions is implemented and the energy exchange between vibrational and translational temperature is based on Landau-Teller non-equilibrium equation, with average relaxation times taken from the Millikan-White (1963) theory modified by Park (1993). The viscosity coefficient for the single specie is computed by means of Yun and Mason (1962) collision integrals, while the conductivity coefficient using Eucken's law. These coefficients for the gas mixture are calculated using semi-empirical Wilke formulas. Diffusion coefficients are obtained by Yun and Mason tabulated collision integrals (1962).

From the numerical point of view, the code is based on a finite volume approach with a cell centered formulation. The inviscid fluxes are computed by Flux Difference Splitting scheme (Borrelli, 1990) and second order approximation is obtained with an Essentially Non Oscillatory (ENO) reconstruction of interface values. Time evolution is performed by an explicit multistage Runge-Kutta algorithm coupled with an implicit evaluation of the chemistry and vibration source terms.

To take into account the effects of rarefaction, slip boundary conditions have been employed. From the large number of available formulations of this kind of conditions, the one proposed by Kogan (1969) has been chosen. These boundary conditions have been obtained by matching the solution of Boltzmann equation in the Knudsen layer to the solution of the macroscopic Navier-Stokes equations, thus yielding:

$$V_s = 1.012\lambda \left(\frac{\partial V_\tau}{\partial n} \right)_w \tag{1}$$

$$T_s - T_w = 1.73 \frac{\gamma}{\gamma - 1} \frac{\sqrt{\pi}}{4} \lambda \left(\frac{\partial T}{\partial n} \right)_w \tag{2}$$

where V_S is the "slip velocity" and T_S the "slip temperature".

2.2 Direct Simulation Monte Carlo method

The Direct Simulation Monte Carlo (DSMC) software used in this paper is the DS2V code of Bird (1995) which is briefly described in the following.

The DSMC method (Bird, 1994) considers the gas as made up of discrete particles that are represented by millions of simulated molecules; it relies on formulas from the kinetic theory of gases. Movement and evolution of each molecule in the simulated physical space is produced by collisions with other molecules and with the body under study, in both cases exchanging momentum and energy. Excitation of rotational and vibrational degrees of freedom and chemical reactions (if any) can be also taken into account.

The computational domain, including the test body, is divided in cells; these are used only for sampling the macroscopic properties and for selecting the colliding molecules. Movement of each molecule from a cell to another one is the product of the velocity (that is the resultant of the convective and thermal velocities) and a time step.

Macroscopic thermo-fluid-dynamic quantities of the flow field (density, temperature, pressure and so on) are computed in each cell as an average over the molecules.

DS2V uses transient subcells in which a transient background grid is built on a single cell and the collision routine, based on nearest-neighbor collisions, is applied. The resolution of the transient grid depends on the number of simulated molecules and, approximately, one simulated molecule corresponds to one subcell.

DS2V provides in output, during the run, the ratio of the local mean separation between collision partners to the local mean free path (mcs/λ). This parameter is indicative of the quality of a run; it should be less than unity every where in the computational domain. Bird (1994, 1995) suggests the value of 0.2 as a limit value.

The present applications rely on the fully accommodated Maxwell gas-surface interactions.

3. Results and discussion

3.1 Hollow cylinder flare test case

In order to validate the methodologies for the prediction of local effects of rarefaction in hypersonic regime and, in particular, concerning the shock wave boundary layer interaction, a typical experimental test case has been selected: the hollow cylinder flare. The hollow cylinder has a sharp leading edge with a bevel angle of 15 deg. The compression flare is inclined of 30 deg with respect to the cylinder and is ended by a hollow cylindrical section. The model total length is 0.17 m and the reference length L is the distance between the leading edge and the beginning of the compression flare. The experiment was carried out in the R5Ch blow-down hypersonic wind tunnel of ONERA at Chalais-Meudon, France by Chantez (1998). A complete numerical Navier-Stokes investigation has been performed by Marini (2002), while a comparison between continuum and kinetic approach compared with experimental results is reported by Markelov (2000). A description of the experiment is briefly reported hereinafter.
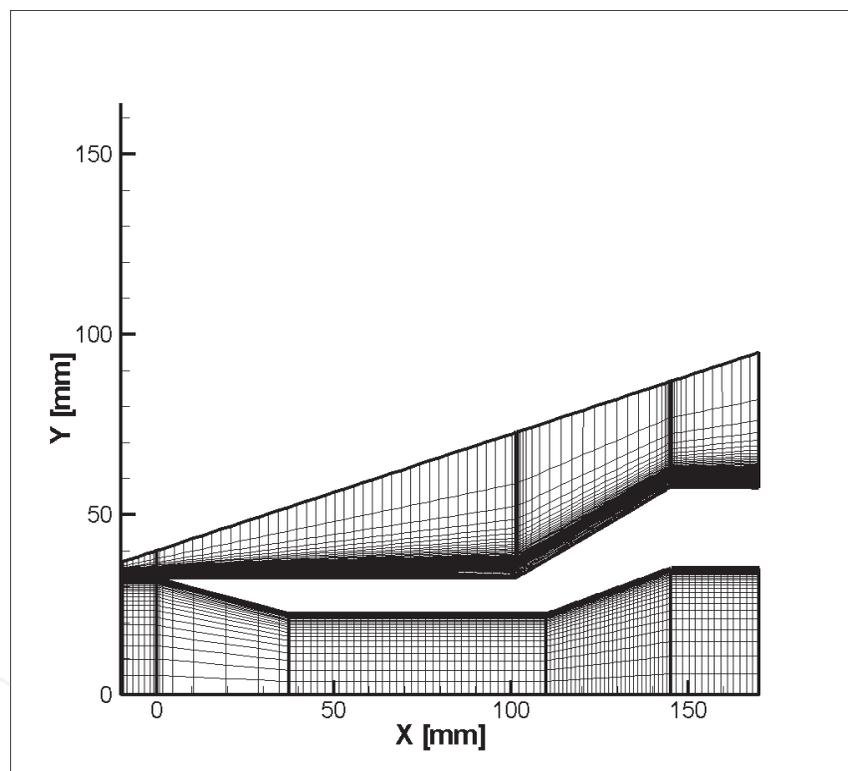
Fig. 2. Validation test case: geometry and computational grid (medium grid level)

The flow conditions for the validation test case are obtained under the nominal stagnation conditions $p_0 = 2.5 \times 10^5$ Pa and $T_0 = 1050$ K, which yield an upstream flow characterized by the following properties: $M_\infty = 9.91$, $Re_\infty/m = 1.86 \times 10^5$, $T_\infty = 51K$ and $p_\infty = 6.3 \, Pa$. The surface temperature of the model is assumed to be constant and equal to $T_w = 293$ K, the Reynolds number based on the reference length L = 0.1017m is equal to $Re_{\infty,L} = 188916$, the mean free path is $\lambda_\infty = 9.5103 \times 10^{-4} \, m$ and the Knudsen number: $Kn_\infty = \lambda_\infty/L = 9.35 \times 10^{-4}$

It is worth to underline that much of the flow domain is in continuum regime except, obviously, the sharp leading edge and the region along the surface where local effect of rarefaction are significant.

A sketch of the geometric configuration is reported in **Fig. 2** together with the computational grid. The following experimental data are available (Chantez et al., 1998): i) pressure coefficient surface distribution (accuracy of 2%); ii) Stanton number (from temperature variations at wall) surface distribution (accuracy of 7%); iii) surface oil-flow visualization (the pattern of skin friction lines over the model indicates the separation and attachment lines, respectively at $X_{sep}/L = 0.76 \pm 0.01$ and $X_{rea}/L = 1.34 \pm 0.015$); iv) flow field visualization by the Electron Beam Fluorescence (EBF) technique; and v) density profile measurements by X-rays detection at the streamwise sections x/L = 0.3; 0.6 (accuracy of 15%) and x/L = 0.76 (accuracy of 8%).

The two-dimensional grid, used for both no slip wall boundary conditions and slip flow ones, is a structured grid composed by 14 blocks, 165888 cells and 169062 points. The grid convergence has been checked.

The location of separation has been used as a parameter to check the needed number of molecules, since it is the most sensitive property to the variation of number of molecules. Table 1 summarizes the performed simulations and shows that the third solution is the converged one.

Solution	Molecules	X_{sep} [mm]
1	8.116×10^6	816.64
2	12.174×10^6	788.24
3	18.258×10^6	787.98

Table 1. Influence of number of molecules on separation

The next **Fig. 3** and **Fig. 4** show the predicted Mach number contour maps and streamlines for CFD with slip boundary conditions and DSMC computations: the strong viscous interaction at the cylinder leading edge appears as well as the evident shock wave boundary layer interaction around the corner, and the subsequent recirculation bubble.
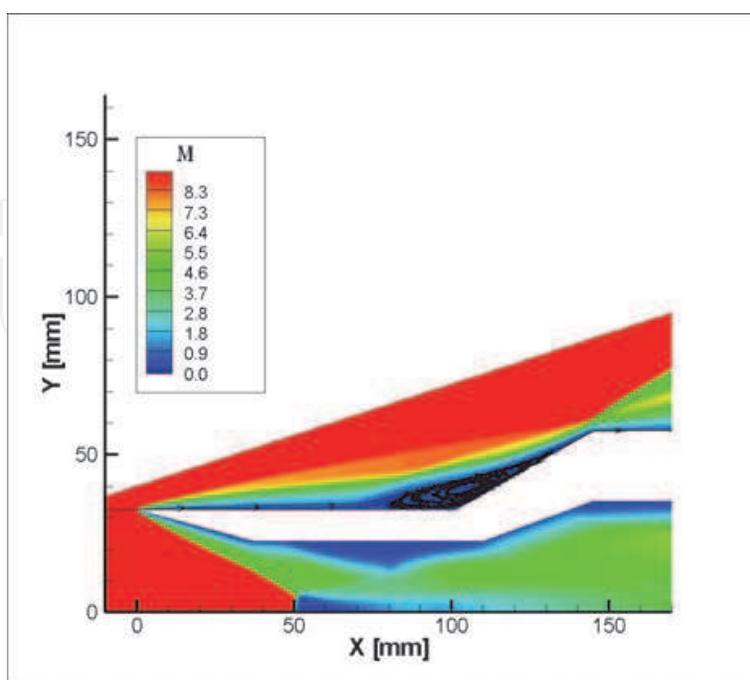

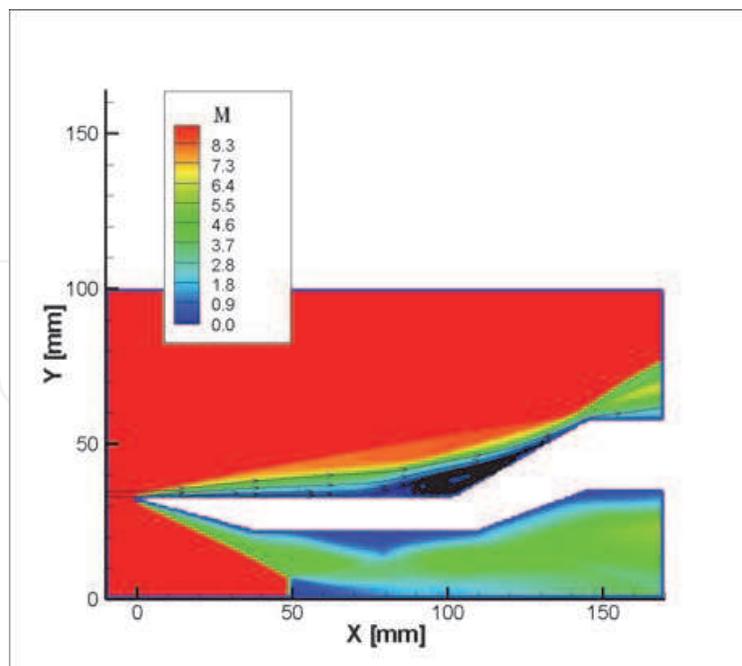Fig. 3. CFD Slip: Mach number contours and streamlines

Fig. 4. DSMC: Mach number contours and streamlines

Fig. 5 displays the normalized slip velocity wall distribution (V_S/V_∞) predicted by DSMC and CFD with the boundary conditions of Equations 1 and 2. In the first part of the wall CFD overestimates the results predicted by DSMC, while downstream of the separation the matching between the two methodologies is rather good.

It is worth to underline that slip velocity along the wall, and in particular ahead of separation location, reaches about 10% of freestream velocity, therefore not negligible rarefaction effects are expected.

Fig. 6 exhibits the pressure coefficient distribution on the wall for the three calculations (CFD No Slip, CFD Slip and DSMC) compared to experimental results. A low initial decrease of pressure coefficient is predicted due to the strong viscous interaction, followed by a first increase of C_p at separation and, then, a strongest one (forty times higher) due to the reattachment shock wave.

DSMC simulation slightly overestimates the experimental pressure coefficient, while both continuum results (CFD No Slip and CFD Slip) show a good agreement with measured values. All computations overestimate the C_p peak at reattachment, and classic CFD is the nearest to the experimental value since at this point the conditions are close to continuum ones, being the local Knudsen number based on boundary layer thickness δ, evaluated as:

$$Kn_\delta = \lambda/\delta \approx 5.28 \times 10^{-3}$$

The analysis of skin friction distribution (**Fig. 7** and **Fig. 8**) shows a different prediction of the three used methodologies for the location of separation. In particular, the predicted separation length is larger as the "*amount of rarefaction of the method*" decreases. In fact, the value of X_{sep}/L for CFD No Slip, CFD Slip and DSMC, is respectively 0.7245, 0.7555 and 0.7748. The experimental value (0.76) is included between CFD Slip and DSMC values as a proof of the local effects of rarefaction, being the local Knudsen number:

$$Kn_\delta = \lambda/\delta \approx 2.17 \times 10^{-2}$$

Note that the reattachment point is not significantly affected by the computation methodology (**Fig. 7**).
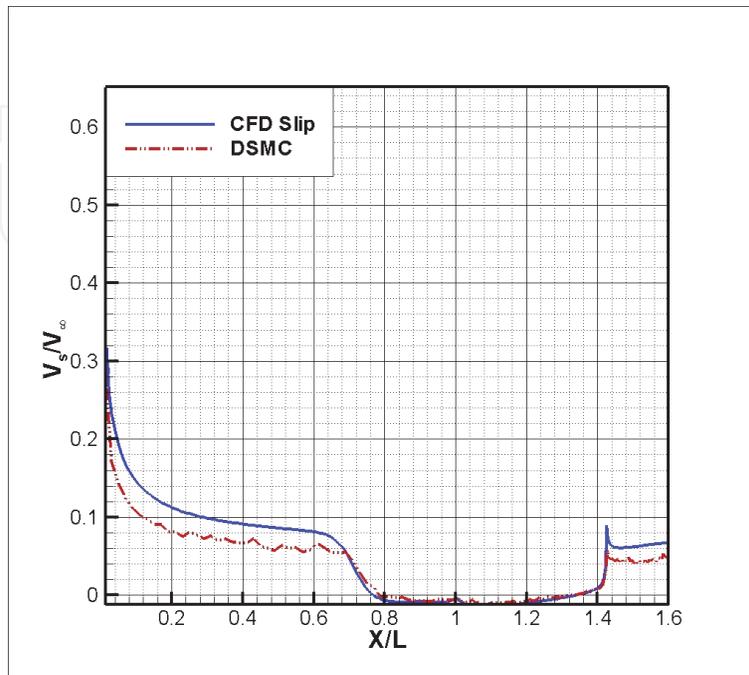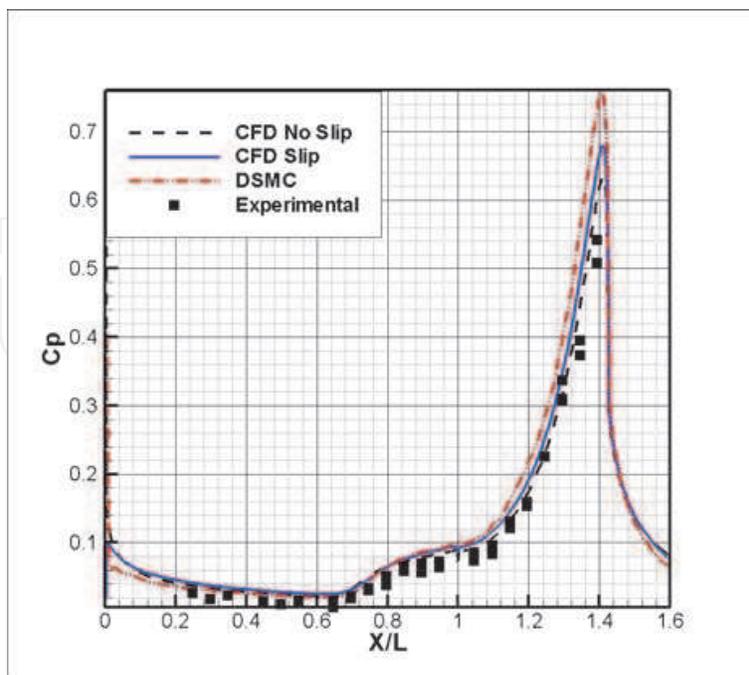

Fig. 5. Slip velocity distribution

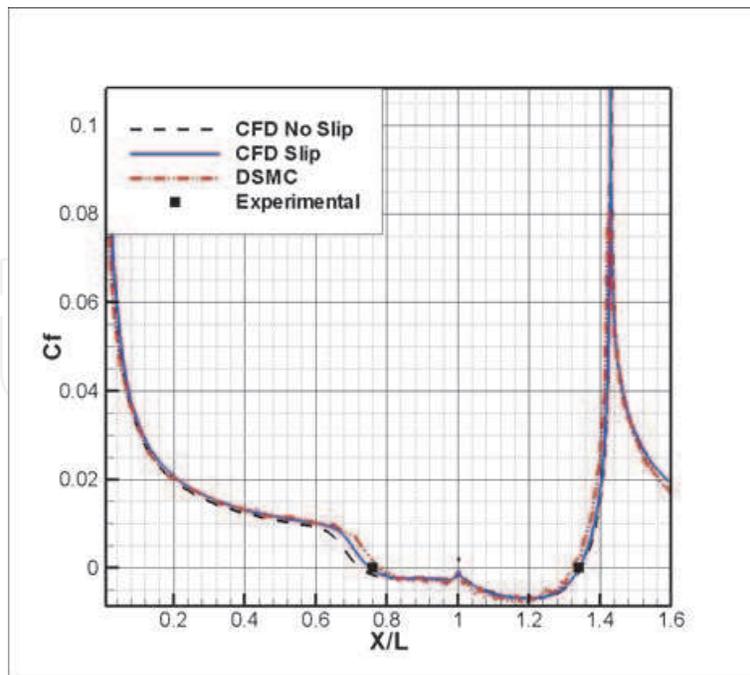Fig. 6. Pressure coefficient distribution

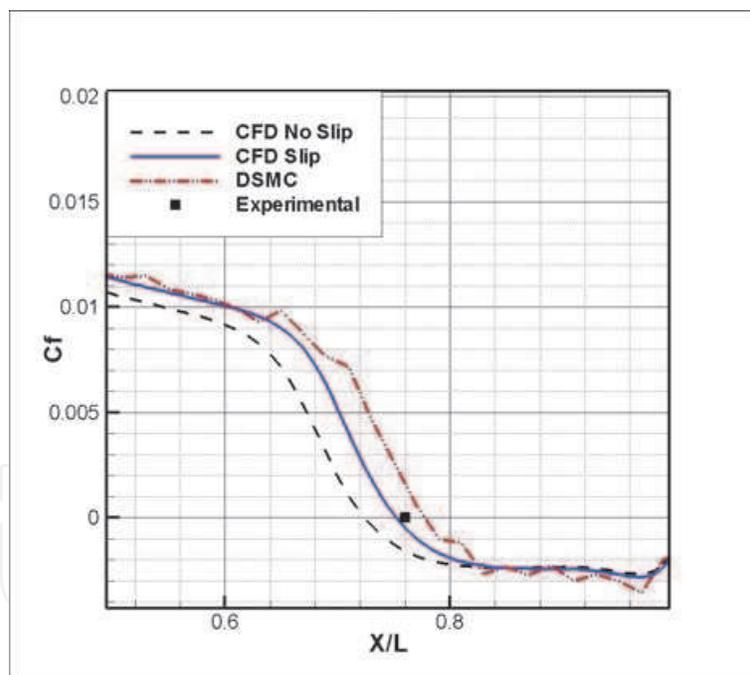Fig. 7. Skin friction coefficient distribution

Fig. 8. Skin friction coefficient distribution (zoom)

The same considerations made in the analysis of skin-friction and pressure coefficients apply to the Stanton number distribution (see **Fig. 9**).

Note that on the leading edge Navier-Stokes with classic boundary conditions (CFD No Slip) overestimates the Stanton number, in fact in this region the boundary layer thickness δ is of the same order of magnitude of the mean free path λ, so

$$Kn_\delta = \lambda/\delta \approx o(1)$$

and the rarefaction effects are maximum.

A comparison of the results obtained by means of numerical simulations with the measured normalized density profiles inside the boundary layer is reported in **Fig. 10** and **Fig. 11**.

In the cross section X/L=0.3 the correlation between numerical and experimental data in the case of Navier-Stokes with slip flow boundary conditions and DSMC is good, while it is fair for CFD with the classic boundary condition (CFD No Slip). In particular, the shock wave inclination predicted by classic CFD is higher with respect to measured one (compare also the Mach number contours of **Fig. 3** and **Fig. 4**).

At the section X/L=0.76 the three numerical methodologies are closer each other and a good agreement with experimental results has been obtained. Note that the predicted inclination of shock wave is nearly the same.

In conclusion, the analysis of the two density profiles shows that the rarefaction effects, as expected, are more significant in the region near the leading edge.
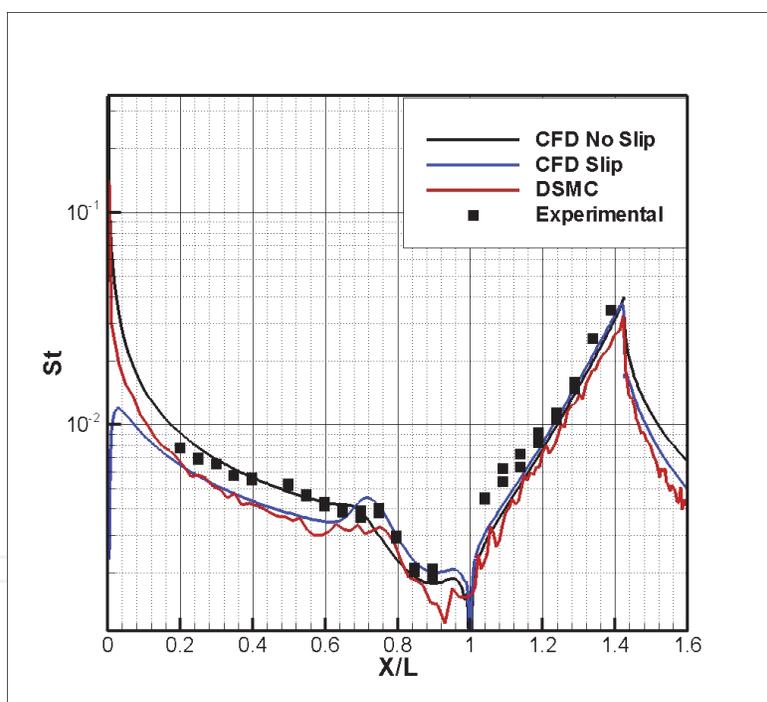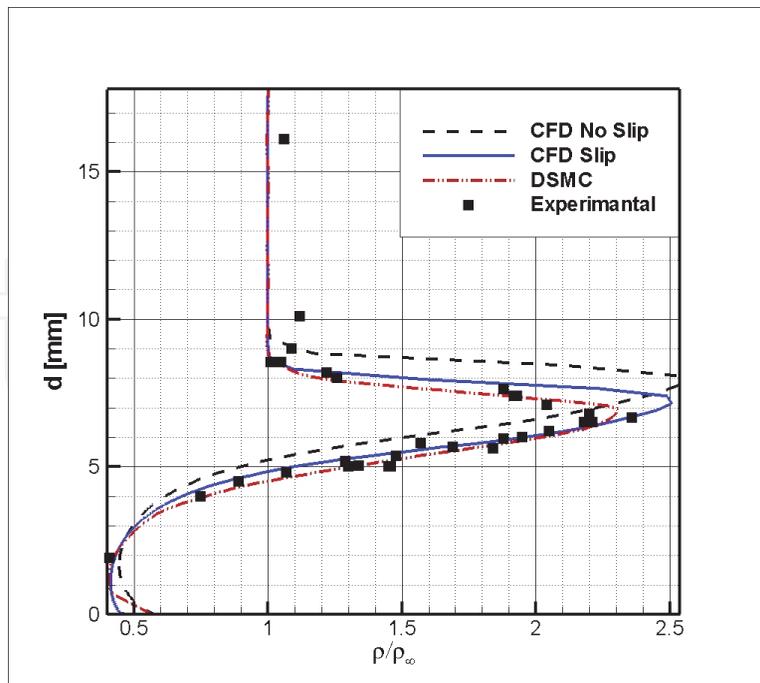

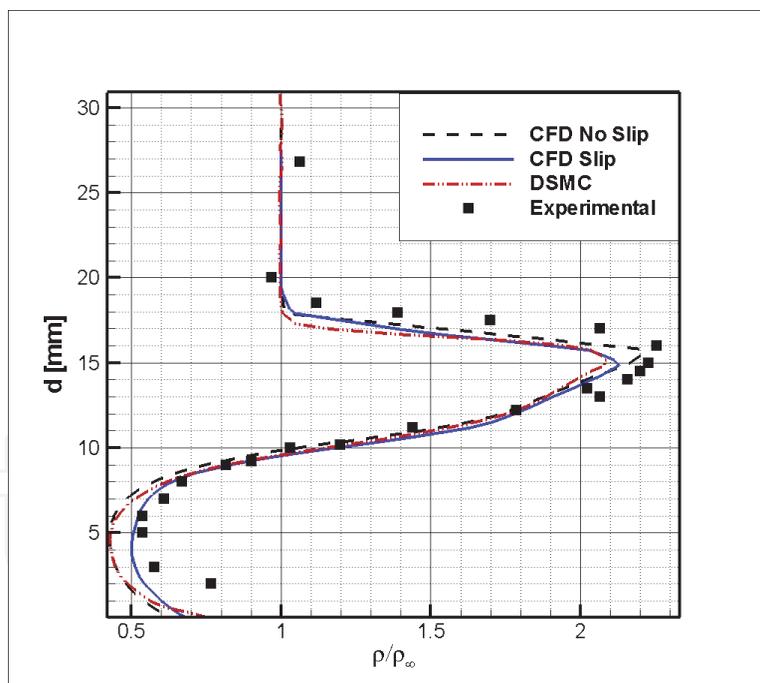Fig. 9. Stanton number distribution

Fig. 10. Density profile: X/L=0.3

Fig. 11. Density profile: X/L=0.76

Finally, the analysis of the present wind tunnel test case simulated with the three different methodologies (classis CFD, CFD with slip flow boundary conditions and DSMC) has shown that local rarefaction effects are significant for the prediction of important aspects of shock wave boundary layer interaction as the sizing of recirculation bubble. Moreover, it has been also shown that CFD with slip flow boundary conditions is, in this case, a good compromise between computational cost and accuracy.

3.2 Scirocco PWT test case

Within the EXPERT program funded by European Space Agency, a number of experiments to be performed in the CIRA Plasma Wind Tunnel "Scirocco", representative of the capsule flight conditions with respect to the shock wave boundary layer interaction phenomenon occurring around the 20 deg open flap, has been designed: PWT driving conditions, model configuration and attitude and model instrumentation have been defined, by means of a massive CFD activity performed by using the CIRA code H3NS, in order to duplicate on a forebody full-scale flap model both pressure and heat flux levels estimated in critical flight conditions.
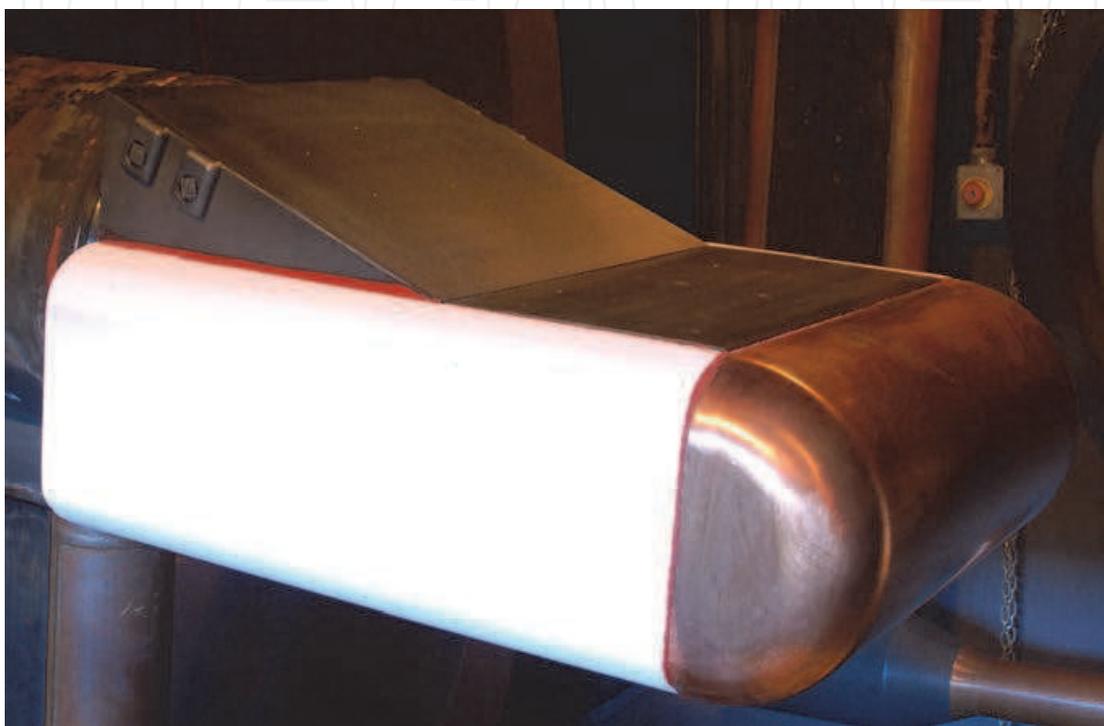
Fig. 12. Model configuration

The model reproduces the EXPERT (Di Clemente et al., 2005) capsule full-scale flap (**Fig. 12**) characterized by 20 deg deflection angle; it is mounted on an holder with a flat plate ahead of the flap with rounded leading and lateral edges. In order to be consistent with the EXPERT capsule, the model will be built by using as much as possible the same materials: in particular, considering the zone of our interest, the upper part is covered by a flat plate of PM1000 (or similar material) equipped with pressure taps, thermocouples and combined heat flux/pressure sensors, whereas the flap is covered by a 4mm thick plate of C-SiC with a deflection angle of 20 deg with respect to the flat plate, and it is equipped with pressure taps and thermocouples. The cylinder leading edge has a radius of 100 mm and a length of 400 mm, the flat plate is 400 mm wide and 200 mm long, the flap is 400 mm wide and 300 mm long. All the lateral edges are rounded with a radius of 50 mm in order to avoid localized over heating, whereas the flap C-SiC plate has a radius of curvature at the lateral edges equal to 4mm (i.e. its thickness). Detailed 2D and 3D computations of the flow around the model with proper thermal and catalytic modeling of the surface have been carried out in different PWT operating conditions determined to duplicate either the SWBLI phenomenon around the body flap either the associated thermo-mechanical loads acting on it during the EXPERT re-entry flight.

For the present qualitative analysis two dimensional computations carried out over the model symmetry plane are taken under consideration; in particular the conditions $H_0=35$ MJ/kg, $P_0=2$ bar are analyzed (this condition corresponding to the lower freestream Knudsen number: $1.47*10^{-3}$) by comparing the results obtained with a classical Navier-Stokes approach and DSMC method, in order to check possible local effects of rarefaction. Note that for this high enthalpy case it has been decided to not perform the CFD slip computation since more accurate DSMC calculations are not strongly CPU-time demanding due to the reduced number of needed particles. Specifically, this test case is characterized by the following flow properties $M_\infty = 12.94$, $Re_\infty/m = 9.03 \times 10^3$, $T_\infty = 240$ K and a model attitude of 12 deg. A grid-independence study for CFD simulations has been carried out as well as a study of DSMC solution sensitivity to the number of particles (not shown).

A preliminary analysis has been carried out considering the wall at fixed temperature of 300 K, and the following **Fig. 13** and **Fig. 14** show the Mach number contours and the streamlines for the two performed computations. Figures show the strong bow shock wave ahead of the model, that is more inclined, as expected, in the case of DSMC simulation, the strong expansion on the bottom part of the model, and finally the shock wave boundary layer interaction around the corner and the subsequent recirculation bubble, that is in incipient conditions in the case of rarefied flow simulation.
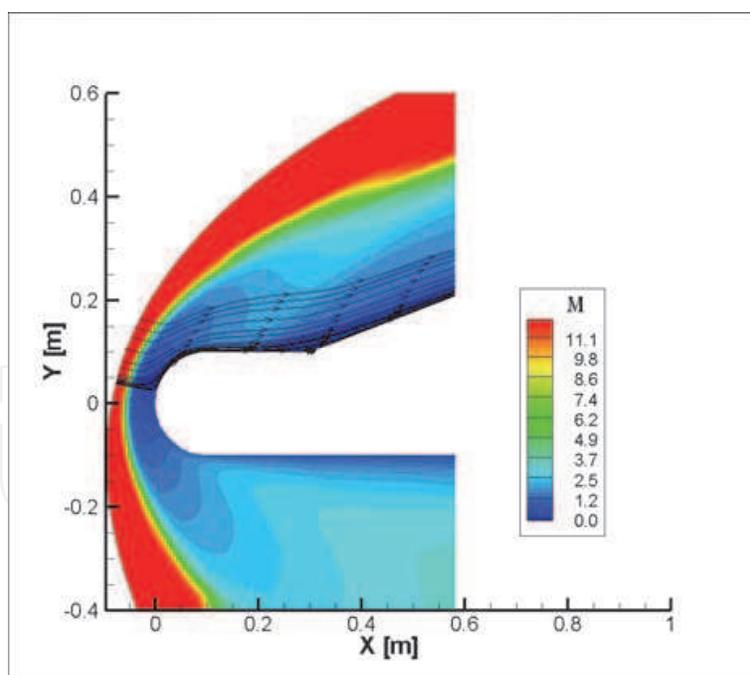

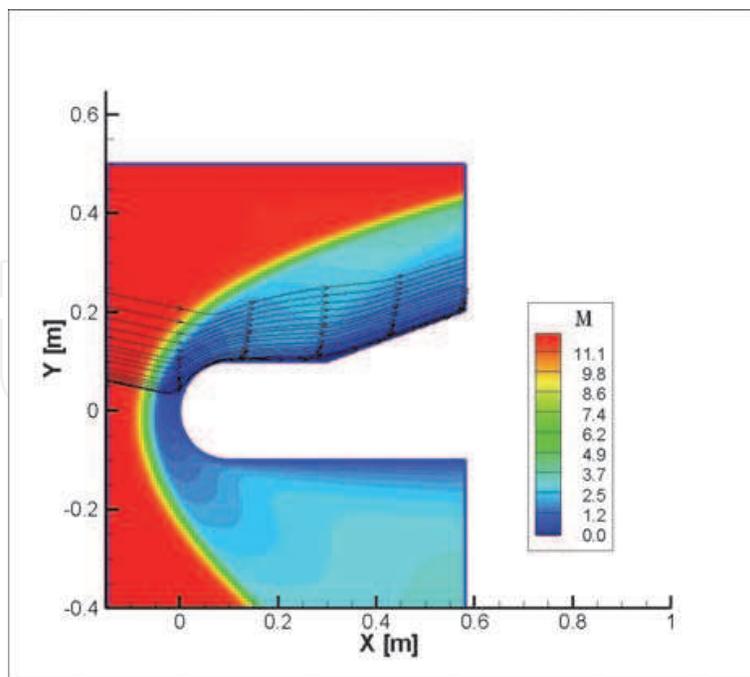Fig. 13. CFD: Mach number contours and streamlines

Fig. 14. DSMC: Mach number contours and streamlines

The **Fig. 15** exhibits the slip velocity wall distribution predicted by DSMC calculation showing a peak value of about 1,3% of freestream velocity in correspondence of the beginning of the flat plate downstream of the model nose. It can be underlined that these low values of slip velocity were expected since, differently from the validation test case (i.e. the hollow cylinder flare), no sharp leading edge is present in this PWT model, therefore *continuum* regime flow conditions are predicted around the nose. Looking also at **Fig. 15** , it can be observed that the same qualitative cuspid-like distribution has been predicted in correspondence of the corner, where a separation (or incipient separation like in this case) occurs.
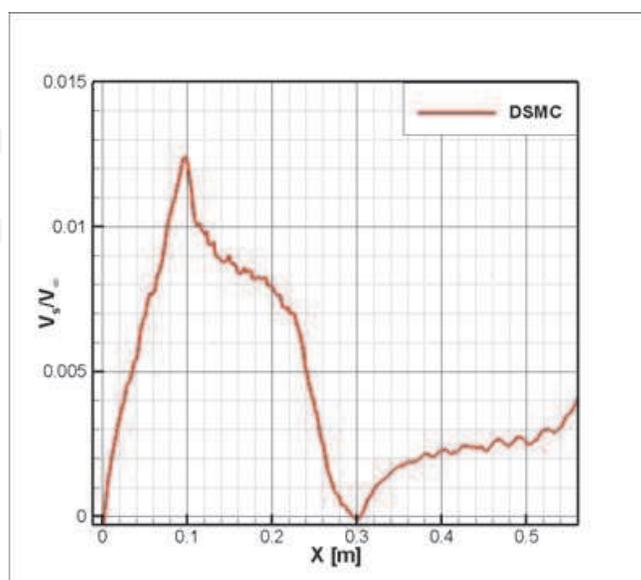
Fig. 15. Slip velocity distribution

By carefully examining **Fig. 16** and **Fig. 17**, and remembering the analysis performed for the validation test case, the same considerations apply to the present applicative case in high enthalpy conditions. In particular, a reduction of separation extent is observed with DSMC calculation (see **Fig. 13** and **Fig. 14**), as well as a slight reduction of the mechanical load acting on the flap (see **Fig. 16**).

Finally, also looking at **Fig. 15**, in correspondence of the section where the maximum of slip velocity occurs, i.e. X=0.1 m, the local Knudsen number is:

$$Kn_\delta = \lambda/\delta \approx 4.05 \times 10^{-2}$$

and this value justifies the occurrence of local effects of rarefaction on the prediction of important aspects of shock wave boundary layer interaction as well as the extent of separation region.
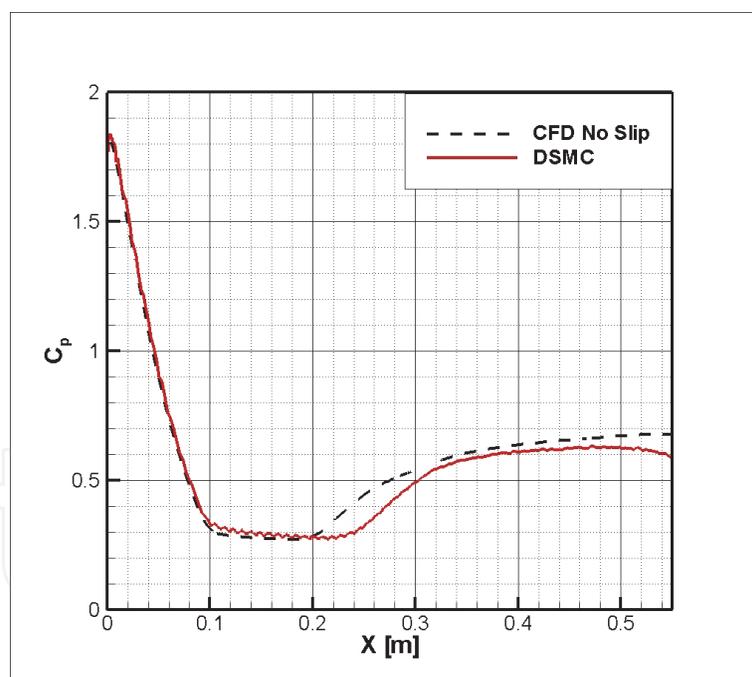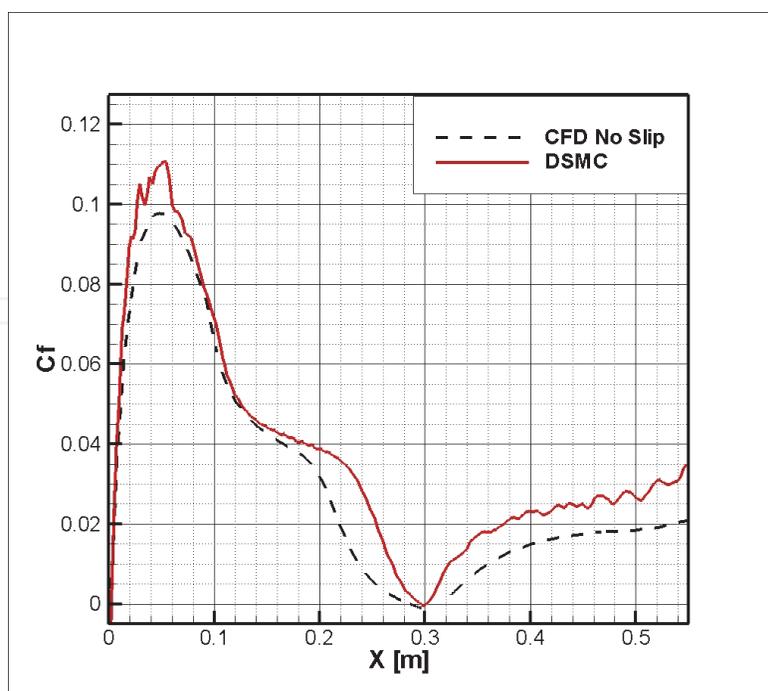

Fig. 16. Pressure coefficient distribution

Fig. 17. Skin friction coefficient distribution

As a conclusion, it must be stressed the fact that local rarefaction effects must be taken into account when designing plasma wind tunnel tests at limit conditions of the facility envelope, in particular for very low pressures and high enthalpies as in the present case.
This is particularly true when plasma test requirements are represented by the reproduction on the test model (or on parts of it) of given values of mechanical and thermal loads, as well as of shock wave boundary layer interaction characteristics (i.e. separation length, peak of pressure, peak of heat flux, etc.).

4. Conclusion

Local effects of rarefaction on Shock-Wave-Boundary-Layer-Interaction have been studied by using both the *continuum* approach with the slip flow boundary conditions and the kinetic one by means of a DSMC code.
The hollow cylinder flare test case for ONERA R5Ch wind tunnel conditions was numerically rebuilt in order to validate the methodologies. The free stream Knudsen number for the selected test case implies that much of the flow is in continuum conditions, even though local effects of rarefaction have been checked. In particular, the comparison with experimental data has shown that rarefactions effects are not negligible in prediction of the separation length. The CFD code with slip flow boundary conditions has shown good predicting capabilities of the size of the recirculation bubble, and the analysis of the density profiles inside boundary layer has shown a good agreement between DSMC and CFD with slip conditions in different sections along the body. Definitively, the present wind tunnel test case, simulated with the three different methodologies (classics CFD, CFD with slip flow boundary conditions and DSMC), has shown that local rarefaction effects are significant for the prediction of important aspects of shock wave boundary layer interaction as the sizing of recirculation bubble and it has been also shown that CFD with slip flow boundary conditions is, in this case, a good compromise between computational cost and accuracy.

The same considerations apply to a CIRA Plasma Wind Tunnel test case, where significant rarefactions effects were found on the SWBLI phenomenon; therefore they must be taken into account when designing plasma wind tunnel tests at limit conditions of the facility envelope, in particular for very low pressures and high enthalpies as in the present case.

5. References

Bird, G. A., Molecular Gas Dynamics and the Direct Simulation of Gas Flows, Clarendon, Oxford, 1994.

Bird, G. A., "The DS2V/3V Program Suite for DSMC Calculations" Rarefied Gas Dynamics, 24th International Symposium, Vol. 762 edited by M. Capitelli, American Inst. Of Physics, NY, 2005, pp. 541-546, February, 1995.

Borrelli S., Pandolfi M., "An Upwind Formulation for the Numerical Prediction of Non Equilibrium Hypersonic Flows", *12th International Conference on Numerical Methods in Fluid Dynamics*, Oxford, United Kingdom, 1990.

Chanetz, B., Benay, R., Bousquet, J., M.,Bur, R., Pot, T., Grasso, F., Moss, J., Experimental and Numerical Study of the Laminar Separation in Hypersonic Flow", Aerospace Science and Technology, No. 3, pp. 205-218, 1998.

Di Clemente M., Marini M., Schettino A., "Shock Wave Boundary Layer Interaction in EXPERT Flight Conditions and Scirocco PWT", 13th AIAA/CIRA International Space Planes and Hypersonics Systems and Technologies Conference, Capua, Italy, 2005.

Kogan N. M., *Rarefied Gas Dynamics,* Plenum, New York, 1969.

Markelov, G., N., Kudryavtsev A. N., Ivanov, M., S., "Continuum and Kinetic Simulation of Laminar Separated Flow at Hypersonic Speeds", The Journal of Spacecraft and Rockets, Vol. 37 No. 4, July-August 2000.

Marini, M., "H09 Viscous Interaction at a Cylinder/Flare Junction", Third FLOWNET Workshop, , Marseille, 2002.

Millikan R.C., White D.R., "Systematic of Vibrational Relaxation", The Journal of Chemical Physics, Vol. 39 No.12, pp. 3209-3213, 1963.

Park C., "A Review of Reaction Rates in High Temperature Air", AIAA paper 89-1740, June 1989.

Park C., Lee S.H., "Validation of Multi-Temperature Nozzle Flow Code NOZNT", AIAA Paper 93-2862, 1993.

Ranuzzi, G., Borreca, S., "CLAE Project. H3NS: Code Development Verification and Validation", CIRA-CF-06-1017, 2006.

Yun K.S., Mason E. A., "Collision Integrals for the Transport Properties of Dissociating Air at High Temperatures", *The Physics of Fluids*, Vol. 39 No.12, pp. 3209-3213, 1962.
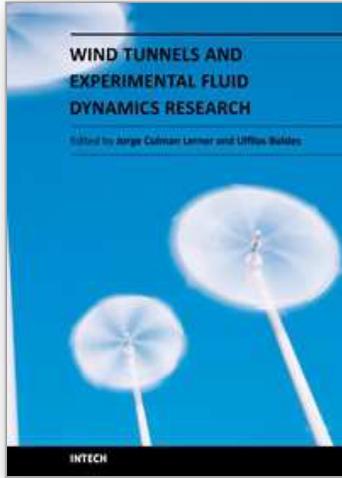
Wind Tunnels and Experimental Fluid Dynamics Research

Edited by Prof. Jorge Colman Lerner

ISBN 978-953-307-623-2

Hard cover, 709 pages

Publisher InTech

Published online 27, July, 2011

Published in print edition July, 2011

The book "Wind Tunnels and Experimental Fluid Dynamics Research" is comprised of 33 chapters divided in five sections. The first 12 chapters discuss wind tunnel facilities and experiments in incompressible flow, while the next seven chapters deal with building dynamics, flow control and fluid mechanics. Third section of the book is dedicated to chapters discussing aerodynamic field measurements and real full scale analysis (chapters 20-22). Chapters in the last two sections deal with turbulent structure analysis (chapters 23-25) and wind tunnels in compressible flow (chapters 26-33). Contributions from a large number of international experts make this publication a highly valuable resource in wind tunnels and fluid dynamics field of research.

INTECH
open science | open minds